Scanning Tunneling Microscopy of Metal Phthalocyanines: d^6 and d^8 Cases

Xing Lu and K. W. Hipps*

Department of Chemistry and Materials Science Program, Washington State University, Pullman, Washington 99164-4630

Received: February 28, 1997; In Final Form: April 28, 1997[⊗]

Scanning tunneling microscopy (STM) images of iron(II) phthalocyanine (FePc) and nickel(II) phthalocyanine (NiPc) adsorbed on the Au(111) surface are reported. Both species provide images showing submolecular structure. A particularly exciting aspect of this work is the strong influence of the metal ion valence configuration on the observed tunneling images. Unlike NiPc, wherein the central metal appears as a hole in the molecular image, the iron ion in FePc is the highest point (about 0.25 nm) in the molecular image. These data are interpreted as indicating that the Fe(II) d^6 system has significant d orbital character near the Fermi energy while the Ni(II) d^8 system does not. This interpretation is consistent with theoretical calculations that predict a large contribution of iron d orbitals near the Fermi energy. The results reported here are also fully consistent with our previous report of CoPc and CuPc d orbital dependent images. An intriguing aspect of this work is that it may be possible to chemically identify different metal complexes simply by their appearance. Metal−organic complex systems of this type may also be viewed as single molecular electronic structures with different parts of the same molecule behaving as insulator, conductor, or semiconductor.

Introduction

Metal(II) phthalocyanines are planar complexes with a structure shown schematically in Figure 1. They are of great technological and fundamental interest, both because of their own properties and because of their similarity to other classes of compounds. Recent theoretical studies of the electronic structure of metal phthalocyanines include, but are not limited to, density functional treatments,[1,2] unrestricted (open shell) Hartree−Fock calculations,[3] multiconfiguration SCF,[4] and extended Huckel MO based elastic scattering quantum chemical calculations.[5] The phthalocyanines are extensively used as pigments and dyes, and they are models for biologically important species such as porphyrins, hemoglobin, and chlorophyll. They can serve as the active elements in chemical sensors, especially for the detection of NO_2.[6,7] They are of great interest for use in optoelectronic devices[8] and solar cells.[9] Their catalytic properties have been studied for some time,[10] most recently for redox catalysis such as in fuel cell applications.[11−13] They are semiconducting and can be used to form well-behaved field effect transistors.[14,15] An understanding of the interaction between metal phthalocyanines (MPc) and surfaces is a critical element required for optimizing their use in many of the applications listed above. Of particular interest are the nature of the bonding between the MPc and the support as reflected in the electronic charge distribution and the geometric configuration of the MPc−support entity. Both of these issues can, in principle, be addressed by obtaining submolecular resolution images of MPc adsorbed on the substrate of interest. Until now, however, only limited information about the chemical nature of the adsorbed MPc was extracted by STM studies.

STM images of individually distinguishable copper phthalocyanine (CuPc) molecules have been presented by a number of researchers. Gimzewski and co-workers studied CuPc adsorbed on polycrystalline silver.[16] Moeller and associates observed single molecules of CuPc on GaAs(110).[17] Lippel et al. reported excellent submolecular resolution images of CuPc adsorbed on Cu(100).[18] Ludwig and associates found highly resolved images of CuPc could be obtained on graphite and MoS_2.[19] Kanai et al. studied CuPc on Si(100) and Si(111).[20] Fritz and co-workers studied hetero-epitaxial layers of CuPc on Au(111),[21] as did Petracek.[22] In addition, images of the free acid (H_2Pc) co-adsorbed on graphite with a liquid crystalline carrier have also been published by Freund and associates.[23] While there have been reports of PbPc studied by STM, no molecular images have been observed.[24,25] In all of these cases, the predominant features of the molecular image could be understood on the basis of the organic material alone. Theoretical calculations of the STM image of CuPc predict that there should be an apparent hole in the center of the molecule,[5−18] and this is what is normally observed.[18,21] Even for H_2Pc, there is an apparent hole in the center of the molecule.[23] The explanation for these "holes", it seemed to us, was that both the occupied and unoccupied orbitals localized on Cu lay more than 1 eV from the Fermi energy, while the MPc ligand LUMO lay close to the Fermi energy.[26,27] We reasoned that as the metal in a MPc system is varied, the corresponding variation in metal d orbital participation near the Fermi surface should produce profound changes in the STM images. Alternatively, dramatic changes in the apparent molecular shape might also occur in systems where interactions between the metal d orbitals and a metallic substrate were significant. In the latter case, the metal surface

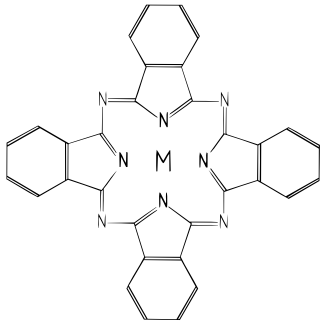

Figure 1. Molecular structure of a typical metal(II) phthalocyanine. The nitrogens that actually bond with the metal ion are shown in intense black.

* Author to whom correspondence is to be addressed.
[⊗] Abstract published in *Advance ACS Abstracts,* June 15, 1997.

S1089-5647(97)00744-X CCC: $14.00

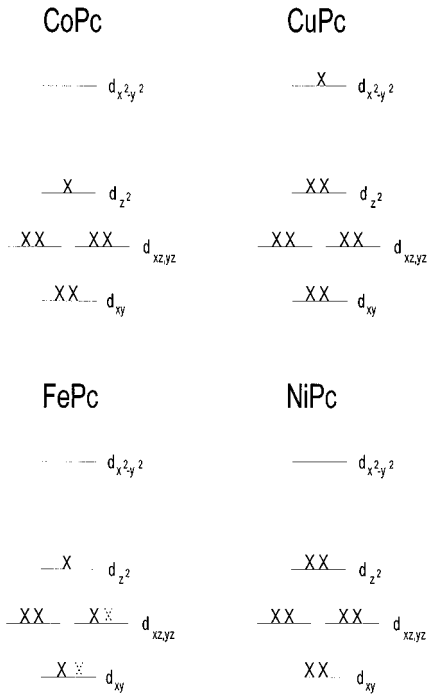

Figure 2. Schematic orbital energy diagram for several transition metal phthalocyanine complexes. In the case of iron(II), a single orbital configuration cannot be used to describe the ground state, and at least two configurations are required. This situation is represented diagramatically by use of a broken × to indicate partial occupation of an orbital by an electron, while a full × represents near complete occupation by a single electron. This diagram is based on ref 1, 3, 30, and 31.

density of states might "shine through", giving enhanced height to the central metal.

As a test of this concept, a study of various metal phthalocyanines was initiated. The first systems chosen were cobalt(II) phthalocyanine (CoPc) (cobalt has a d^7 configuration) and CuPc (d^9 configuration). Calculations[1,3] show that the CoPc d_{z^2} orbital is roughly half filled and lies very near the ligand HOMO. Rosa's calculations place the filled CuPc d_{z^2} orbital about 2 eV below the ligand HOMO, and there is no significant d orbital contribution within a band 1 eV above and 2 eV below the ligand HOMO in CuPc.[1] Our recently reported STM images of CoPc and CuPc on Au(111) are fully consistent both with our hypothesis of d orbital dependent STM images and with these theoretical results.[28,29] STM images of CoPc and CuPc show that CuPc molecules have an apparent hole in the center of the ring, while CoPc units have what appears to be a very tall atom in the center. On the basis of crude orbital energy arguments[30,31] (see Figure 2) and the expectation that tunneling from the metal substrate to the STM tip will be most enhanced when the orbitals have a spatial distribution consistent with carrying charge from below to above the molecular plane, the apparent height of Co(II) relative to the Cu(II) in MPc complexes is easily rationalized as due to the half-filled d_{z^2} orbital.

On the basis of these arguments, FePc and NiPc should show contrasts similar to that observed for CoPc and CuPc, respectively. Thus, one of our goals in this paper is to demonstrate that the submolecular resolution images of FePc and NiPc behave as predicted. Another issue to be addressed here is the possible role of O_2 in the image formation mechanism. While all of our MPc images have been collected under conditions where the partial pressure of O_2 is less than 5×10^{-11} Torr, the CoPc and CuPc samples reported previously were made in one UHV chamber and then transferred in air to another. In this work we will contrast FePc films made in the above manner with those where the FePc film is deposited inside the STM vacuum chamber such that the O_2 partial pressure is never higher than 5×10^{-11} Torr throughout the deposition or subsequent STM imaging.

Experimental Section

The metal phthalocyanines were purified by multiple sublimation before use. The gold was purchased from Cerac and was 99.999% purity. Mica sheets were purchased from Ted Pella and were freshly cleaved just before use. In a single continuous operation, 0.2−0.4 nm of FePc or NiPc were deposited onto either a 80 nm or 300 nm thick layer of Au(111) epitaxially grown on mica. The Au(111) was grown in a cryopumped chamber having a base pressure of $\leq 3 \times 10^{-9}$ Torr. In detail, the mica was heated to 550 °C in vacuum for a period of 2 h and then allowed to cool to 375 °C. The Au layer was deposited onto the mica (still at 375 °C) at a rate of 7.8 nm/min as measured by a quartz thin film monitor. The substrate was then allowed to cool, and one of two preparative schemes was used to prepare the MPc layer. In the first method, the Au film was cooled to either 180 or 50 °C and, without breaking vacuum, the MPc was vapor deposited at a rate of 1.8 nm/min from an ME-1 source (R. D. Mathis). These samples were then allowed to cool to room temperature in vacuum, removed from the prep chamber, and then rapidly transferred to the UHV chamber housing a McAllister STM. We will identify films prepared by this first method as *once exposed to air*. In the second method, the freshly prepared Au films were cooled to room temperature, removed from the prep chamber, and inserted (via load lock) into the STM vacuum chamber. In this case FePc films were deposited inside the STM vacuum chamber while monitoring the O_2 partial pressure with a quadrupole mass spectrometer. We found that the oxygen level never rose higher than 5×10^{-11} Torr throughout the deposition and subsequent STM imaging.

Both W and Pt/Ir tips were used for STM analysis. The W tips (0.5 mm in diameter) were electrochemically etched in 1.0 M KOH using about 30 V ac, while the Pt/Ir tips (0.25 mm in diameter) were cut with scissors. Once the tips were in vacuum, they were cleaned by electron bombardment from a hot filament. Typically 4 mA of current at 1000 V was passed through each tip for a period of 30 s. The McAllister STM is based on the slip-stick principal and is controlled by a Digital Instruments Nanoscope III. Typical images were acquired in constant current mode at a scan rate of 2−6 Hz. High bias/low current (±0.8 V/300 pA) and low bias/high current (±0.1 V/2 nA) conditions were used depending upon the tip and sample. The images were manually plane-fit to account for sample tilt and then either low-pass filtered or Fourier filtered. In either case, the Nanoscope III software (version 3.2) was used. If not otherwise indicated in the figure caption, only plane fitting and low-pass filtering were applied.

We also took advantage of the current imaging tunneling spectroscopy (CITS) option built into the Nanoscope hardware. Thus, an array of 32 × 32 current−voltage ($I-V$) curves were acquired while a 256 × 256 image was also obtained. Due to poor timing between $I-V$ and image scan lines and the lack of averaging capability for the $I-V$ curves, the CITS data (both image and $I-V$ curves) are fairly noisy.

Results and Discussion

A 0.3 nm layer of a metal(II) phthalocyanine on Au(111) forms a near monolayer. While it is easy to observe the individual molecules as fuzzy disks by STM, it is more difficult

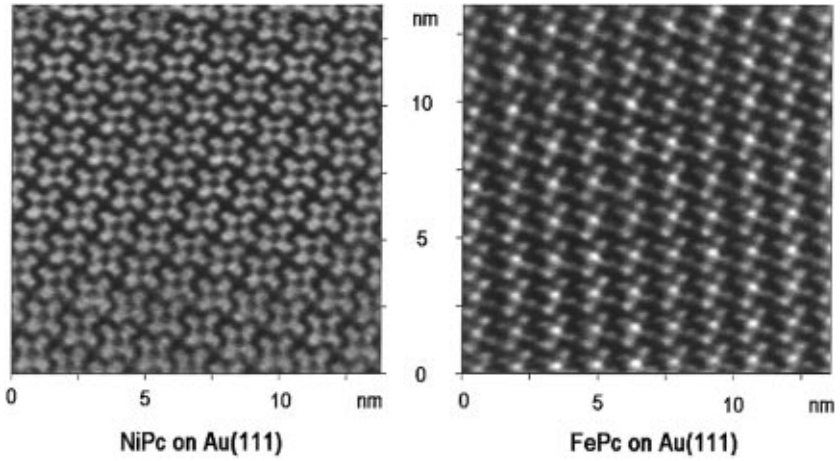

Figure 3. Top view STM images of a 0.4 nm thick layer of NiPc and of 0.3 nm of FePc on Au(111) obtained with a W tip. Both samples had MPc layers that had once been exposed to air. The gray scale extends over 0.3 nm. For NiPc the sample bias was +0.50 V and the tunneling current was 300 pA. For FePc the sample bias was +0.10 V and the tunneling current was 1.6 nA. The image was Fourier filtered to reduce noise.

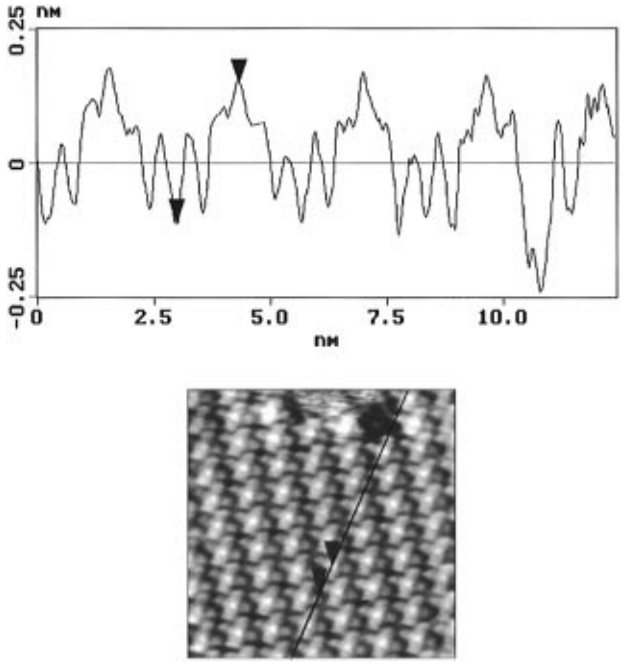

Figure 4. Top view and sectional STM image of a 0.3 nm thick layer of FePc adsorbed on Au(111). The FePc was once exposed to air. The image was obtained with a PtIr tip at a sample bias of +0.15 V and a fixed tunneling current of 300 pA.

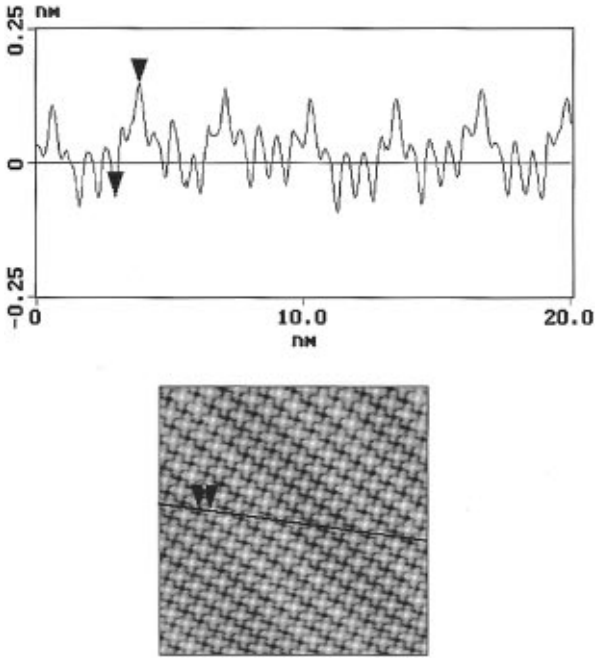

Figure 5. Top view and cross sectional plot of a 0.2 nm thick FePc film on Au(111) prepared and measured in the STM UHV chamber. A Pt−Ir tip was used at a sample bias of −0.50 V and a current of 400 pA.

to resolve structure on the submolecular scale. Figure 3 presents good quality images of both NiPc and FePc that had once been exposed to air (see the Experimental Section). The four leaf pattern of the phthalocyanine ring is clearly observed, as is the depression (dark area) in the center of every NiPc molecule. On the other hand, the center of every FePc has a large hill (bright spot). Similar results have also been obtained with Pt/Ir tips and a variety of bias voltages and currents. The FePc images were always highest in the center, while the NiPc images always appear to have holes where the Ni(II) should be.

A sectional cut of another FePc sample (once exposed to air) shows the detailed variation with height observed as a function of position over the FePc. As seen in Figure 4 the cross section was chosen to pass through the center of an FePc molecule (bottom center of image), across the benzene rings of two different arms of adjacent FePc's, and again through the center of another FePc, in a repeating pattern. In this image, the benzene rings all appear of roughly equal height (about 0.17 nm) and somewhat taller than the carbons of the five-member rings and the peripheral (noncoordinating) nitrogens. The Fe^{2+} ion region appears to be about 0.25 nm high, defining the total molecular height. Of course, the apparent height depends on a number of parameters including, but not limited to, the sharpness of the tip and the sample−tip separation. These will be discussed in more detail later.

To address the issue of possible oxygen contamination during sample transfer between UHV systems, several FePc films were deposited in situ. That is, they were deposited in the UHV chamber that houses the STM and never exposed to more than 5×10^{-11} Torr of O_2 during preparation, handling, or measurement. An example of the results obtained from such films is presented in Figure 5, wherein both a top view and sectional view are shown. While the maximum height of the FePc now appears to be about 0.20 nm, the benzene rings now appear only about 0.11 nm tall, making the relative height of the central metal even greater than in the once air exposed sample. Moreover, the relative resolution is clearly better than in Figure 4, since the drop in apparent height over the inner carbon atoms

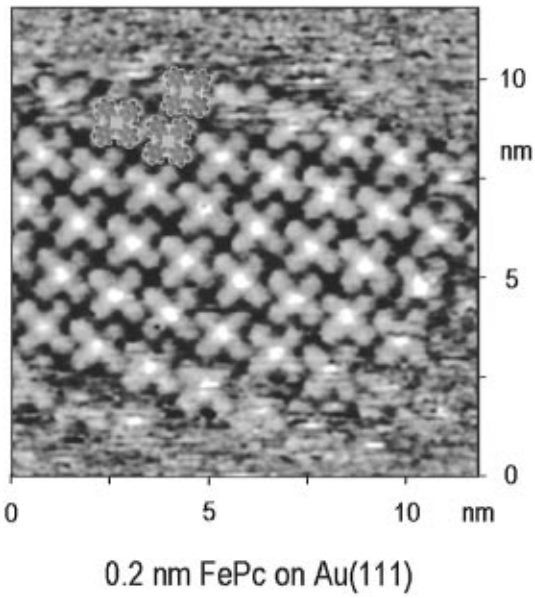

Figure 6. Top view of a small FePc island on a Au(111) surface. The inset shows three space-filling models of a typical MPc. A Pt−Ir tip was used at a sample bias of −0.50 V and a current of 200 pA.

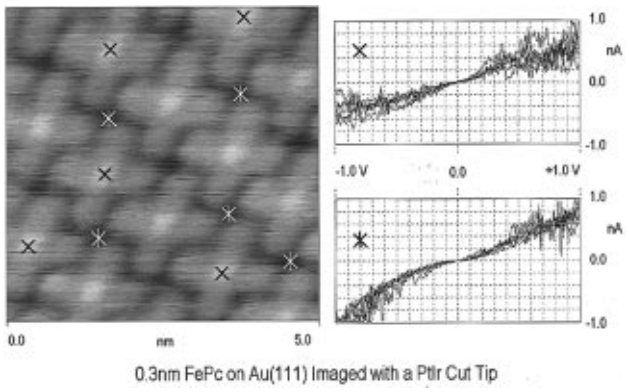

Figure 7. *I*−*V* curves and simultaneous top-view image of FePc adsorbed on Au(111). The curves associated with × correspond to the marked positions of iron(II) ions. The curves associated with * correspond to the indicated areas between FePc molecules. The data were obtained with a Pt−Ir tip, and the starting point for *I*−*V* curves was set by a bias of −0.50 V and a current of 300 pA.

and the noncoordinating nitrogens is more clearly observed. The underlying undulation in the image is believed to be due to reconstruction of the gold surface.

The height of the molecule above the gold layer is actually greater than determined from measurements over the ordered region alone. The tip is seldom sharp enough to allow the tunneling current to come only from the Au surface in the region between molecules. In the "low" regions between MPc molecules, current comes both from the Au surface and from a portion of the MPc in close proximity to the tip edges. Even measuring heights at island edges is somewhat problematic because the "exposed" gold surface is actually partially covered. If we image a small FePc island, as is shown in Figure 6, we see two-phase coverage with a 2-D solid surrounded by a 2-D fluid. What appears to be a noisy Au surface is actually caused by molecules moving about under the tip. Moverover, the island edges are constantly changing with both the addition and loss of molecules, as can be seen from the partial molecular images present in Figure 6 at the edges of the island.

The MPc height values reported here are significantly smaller than the interplanar spacing in crystalline MPc's: about 0.38 nm in the α form.[32] On the other hand, the heights observed over the benzene rings are fairly close to what is expected for a C−C bond in benzene (about 0.14 nm).[33] This argues for a height interpretation based on the atomic diameters of the surface species. On the other hand, the apparent Fe^{2+} (0.25 nm) and the Ni^{2+} (<0.10 nm) heights are clearly not indicative of size in the normal sense since their ionic diameters are 0.144 and 0.140 nm, respectively.[34] Thus, on the basis of electron density alone, there should be no discernible difference between the STM images of FePc and NiPc, and these images should have, at most, a very slight elevation in the molecular center.

It is well-known that both the electron density and the local density of surface states near the Fermi energy play a critical role in determining the STM image.[35,36] STM imaging of electronegative or electropositive elements, for example, can result in the observation of anomalous heights.[37] Another classic example is the observation of the dangling bonds on the silicon surface.[38] It is clear in the present case that the occupancy of the d orbitals is playing a significant role in the STM image. In the simplest possible picture, Fe(II) is acting as a conductor while Ni(II) is not. Since the STM images reflect contours of constant current, the tip must dip toward the Au surface above the Ni(II) center and pull back from the Fe(II) in order to maintain constant current flow. There are, however, at least three separate mechanisms (consistent with our conjecture) that could lead to the observed differences in height. If the tunneling current is primarily LUMO or HOMO mediated, then the bright central region would be due to the half-filled $3d_{z^2}$ and partially filled (d_{xz}, d_{yz}) orbital pair. These are the most likely candidates both by symmetry and since they have the largest projection out of the plane of the molecule. Moreover, these orbitals are located more than 1.3 eV from the Fermi energy in NiPc and are not expected to contribute significantly to the NiPc STM image. In any of these cases, the mechanism for the tunneling enhancement in FePc would be some form of d-orbital-mediated tunneling. This might be through a true resonance process,[39] where the MPc orbital coherently couples to the states of the substrate and tip. Or, it might be an incoherent transient process such as the orbital-mediated tunneling seen in tunnel diodes containing metal phthalocyanines.[26,27]

Alternatively, the unpaired electrons on iron may form a partial bond with the underlying gold, as has been suggested for CoPc on platinum electrodes.[11] This would also provide a mechanism for channeling Au surface electron density through the iron center and then to the tip. This might be similar to the case of Xe on Ni(110), wherein Xe can be imaged because of the very slight residual density of the 6s electron at the Fermi level. This despite the fact that the peak in that resonance lies close to the vacuum state.[40] Enhanced electron density in the d_{z^2} orbital could also lead to the apparent height of the central atom. Higher resolution STM images (the d_{xy}, d_{xz}, and d_{yz} orbitals should all have a small hole in their center) might resolve this issue in cases where only the d_{z^2} orbital is partially occupied, but the results are problematic for the FePc system where all the low lying d orbitals are not fully occupied.

In the context of these two possible models, it should be pointed out that bright areas appear to include the four coordinating N atoms (see Figure 6). This might be an artifact of using a tip that is broader than 1 atom, or it might be that the orbital responsible for the enhanced conduction includes some admixture of p_z orbitals on the coordinating nitrogen atoms. Also, as will be shown in Figure 7, the *I*−*V* curves taken over the iron ions show little or no asymmetry, suggesting either that the critical orbital(s) are very close to the Fermi energy or that both occupied and unoccupied orbitals participate.

A third explanation for the differences in the images of FePc and NiPc would involve the chemical reactivity of the partially filled d_{z^2} orbital. Iron phthalocyanine has been shown to reversibly absorb molecular oxygen at pressures above 2×10^{-7} Torr.[41] Cobalt(II) tetrasulfophthalocyanine (CoTSPc) reacts reversibly with oxygen in water at pH greater than 12 to form a dioxygen adduct.[42,43] Thus, the adsorption of dioxygen on FePc might account for the apparent increase in height of the iron center. This explanation, of course does not account for the hole in the NiPc complex and seems unlikely at the pressure at which these measurements were performed. To address this issue more directly, the results from once air exposed (Figures 3 and 4) and UHV only history samples (Figures 5−7) were compared. Since some of our data were acquired with no more than about 0.03 langmuir of total O_2 exposure, it seems very unlikely that every FePc would have an attached O_2 molecule.[44] It should also be noted that CuPc and NiPc also are reported to adsorb oxygen with saturation coverage occurring at about 3×10^{-8} Torr,[45] yet we have never seen any high spots in either NiPc or CuPc samples. Nevertheless, until an Auger or ESCA measurement can be made in the STM chamber before and after deposition and then after STM imaging, the issue cannot be totally closed. Unfortunately, we do not have the facilities to make such a measurement.

The CITS data, while fairly noisy for reasons indicated in the Experimental Section, do provide some insight into the conduction mechanism. Figure 7 shows the image obtained while regularly but infrequently (one $I-V$ curve for every 64 image points) turning off the feedback and recording an $I-V$ curve. In Figure 7 we have shown six $I-V$ curves obtained near the center of the iron ion in six different MPc molecules and six different regions between FePc molecules. (Only five of the six points are marked because of an artifact in the Nanoscope software.) There is a clear difference in these curves. The $I-V$ curves taken above an Fe^{2+} are approximately linear, while those taken over the exposed gold surface are very nonlinear. In fact, the shape of the * curves are as expected for M−I−M' tunneling, while the iron site curves are more ohmic. While more experimental work is certainly called for, including quieter data taken at a broader range of positions, these results are highly suggestive that the Fe^{2+} ion is indeed acting as some type of atomic wire.

Conclusions

Contrary to the expectations set by past STM studies of CuPc and H_2Pc, more than the Pc^{2-} electronic structure must be considered in any attempt to predict and/or interpret the scanning tunneling microscopy images obtained from a general member of the class of metal phthalocyanines. On the basis of the results presented here, the orbital configuration of the central metal ion must be considered since it can, in certain cases, provide the dominant tunneling pathway for the molecule and in other cases block conduction through regions of a molecule. This issue has special relevance for metal−macrocyclic systems where the metal ion can range through much of the periodic table, providing valence shell orbitals of s, p, d, or even f type, while the π orbital structure of the macrocycle can be varied to provide HOMO and LUMO orbitals of varying energy with respect to the Fermi energy. Since the presence of local orbitals close to the Fermi energy produces large conduction (atomic wires) while local HOMOs and LUMOs far from the Fermi energy result in insulating behavior, single-molecule devices having complex electronic functions could be built from appropriately selected macrocycles. While the Pc ligand itself is a semiconductor because of its relatively narrow HOMO−LUMO gap,[26,27] other macrocycles with larger gaps could be used to make cobalt(II) or iron(II) complexes that were truly two-dimensional insulated wires: a central atomic conductor sheathed in a molecular insulator. One may even speculate about the interesting properties that might be observed for truly molecular electronics composed of conducting, insulating, and semiconducting pieces linked chemically to provide some overall electronic functionality.

The use of mixed MPc adlayers provides us with a new means for studying the processes associated with film formation and diffusion in two dimensions. The use of a small amount of an electronically "hot" species like FePc mixed into an electronically "cold" system like NiPc can provide a mechanism for monitoring surface diffusion processes. Moreover, the detailed distributions of MPc and M'Pc in a mixed film could be used to study other processes such as thermal annealing, 2-D sublimation, and orientational changes with coverage. Another application is in the measurement of relative sticking coefficients.

Acknowledgment. We thank the National Science Foundation for their assistance in the form of grants DMR-9201767 and DMR-9205197. We also thank Professor Ursula Mazur for her assistance.

References and Notes

(1) Rosa, A.; Baerends, E. J. *Inorg. Chem.* **1994**, *33*, 584−595.
(2) Rosa, A.; Baerends, E. J. *Inorg. Chem.* **1992**, *31*, 4717−4723.
(3) Reynolds, P. A.; Figgis, B. N. *Inorg. Chem.* **1991**, *30*, 2294−2300.
(4) Carniato, S.; Dufour, G.; Rochet, F.; Roulet, H.; Chaquin, P.; Giessner-Prettre, C. *J. Electron Spectrosc. Relat. Phenom.* **1994**, *67*, 189−193.
(5) Sautet, P.; Joachim, C.; Bocquet, M. L.; Salmeron, M. *Ann. Chim. (Paris)* **1992**, *17*, 217−227.
(6) Collins, R. A.; Mohammed, K. A. *J. Phys. D* **1988**, *21*, 142−150.
(7) Hamann, C.; Hietschold, M.; Mrwa, A.; Mueller, M.; Starke, M.; Kilper, R. *Top. Mol. Organ. Eng.* **1991**, *7*, 129−136.
(8) Flynn, B. W.; Owen, A. E.; Mayor, J. *J. Phys. C* **1977**, *10*, 4051−4058.
(9) Ghosh, A. H.; Morel, D. L.; Feng, T.; Shaw, R. F.; Rowe, C. A. *J. Appl. Phys.* **1974**, *1*, 20−33.
(10) Kropf, H.; Steinbach, F. *Katalyse an Phthalocyaninen*; Georg Theme Verlag: Stuttgart, 1973.
(11) Mho, S.; Ortiz, B.; Park, S.-M.; Ingersoll, D.; Doddapaneni, N. *J. Electrochem. Soc.* **1995**, *142*, 1436−1441.
(12) Zagal, J. H. *Coord. Chem. Rev.* **1992**, *119*, 89−112.
(13) Thomas, A. L. *Phthalocyanine Research and Applications*; CRC Press: Boca Raton, FL, 1990.
(14) Madru, R.; Guillaud, G.; Sadoun, M.; Maitrot, M.; Andre, J. J.; Simon, J.; Even, R. *Chem. Phys. Lett.* **1988**, *145*, 343−360.
(15) Maitrot, M.; Guillaud, G.; Boudjema, B.; Andre, J. J.; Strzelecka, H.; Simon, J.; Even, R. *Chem. Phys. Lett.* **1987**, *133*, 59−65.
(16) Gimzewski, J. K.; Stoll, E.; Schlittler, R. R. *Surf. Sci.* **1987**, *181*, 267−277.
(17) Moeller, R.; Coenen, R.; Esrlinger, A.; Kaslouski, B. *J. Vac. Sci. Technol. A* **1990**, *8*, 659−660.
(18) Lippel, P. H.; Wilson, R. J.; Miller, M. D.; Woell, C.; Chiang, S. *Phys. Rev. Lett.* **1989**, *62*, 171−174.
(19) Ludwig, C.; Strohmaier, R.; Petersen, J.; Gompf, B.; Eisenmenger, W. *J. Vac. Sci. Technol. B* **1994**, *12*, 1963−1966.
(20) Kanai, M.; Kawai, T.; Motai, K.; Wang, X. D.; Hashizume, T.; Sakura, T. *Surf. Sci.* **1995**, *329*, L619−L623.
(21) Fritz, T.; Hara, M.; Knoll, W.; Sasabe, H. *Mol. Cryst. Liq. Cryst. Sci. Technol. Sect. A* **1994**, *252−253*, 561−570.
(22) Petracek, V. *Int. J. Electron.* **1995**, *78*, 267−272.
(23) Freund, J.; Probst, O.; Grafstroem, S.; Dey, S.; Kowalski, J.; Neumann, R.; Woertge, M.; zu Putlitz, G. *J. Vac. Sci. Technol. B* **1994**, *12*, 1914−1917.
(24) Pester, O.; Mrwa, A.; Hietschold, M. *Phys. Status Solidi A* **1992**, *131*, 19−23.
(25) Hamann, C.; Laiho, R.; Mrwa, A. *Phys. Status Solidi A* **1989**, *116*, 729−734.
(26) Mazur, U.; Hipps, K. W. *J. Phys. Chem.* **1995**, *99*, 6684−6688.
(27) Mazur, U.; Hipps, K. W. *J. Phys. Chem.* **1994**, *98*, 8169−8172.
(28) Hipps, K. W.; Lu, X.; Wang, D.; Mazur, U. *J. Phys. Chem.* **1996**, *100*, 11207−11210.

(29) Lu, X.; Hipps, K. W.; Wang, D.; Mazur, U. *J. Am. Chem. Soc.* **1996**, *118*, 7197−7202.

(30) Scrocco, M.; Ercolani, C.; Paoletti, A. M. *J. Electron Spectrosc. Relat. Phenom.* **1993**, *63* (2), 155−66.

(31) Joswig, H. J.; Schmidt, H. H.; Steinbach, F.; Stritzel, R. *Proc. Int. Congr. Catal., 6th* **1976**, Bond, G. C.; Wells, P. B.; Tompkins, F. C., Eds.; Chemical Society: Letchworth, U.K., 1977; Vol. 1, pp 583−592.

(32) Simone, J.; Andre, J. J. *Molecular Semiconductors*, Springer Verlag: New York, 1985; p 81.

(33) *Tables of Interatomic Distances and Configuration in Molecules and Ions*; Sutton, L. E., Ed.; The Chemical Society: London, 1958.

(34) Segal, B. *Chemistry*, John Wiley and Sons: New York, 1985; p 817.

(35) Stroscio, J. A.; Kaiser, W. J. *Scanning Tunneling Microscopy*, Academic Press: New York, 1993.

(36) Wiesendanger, R.; Guntherodt, H. J. *Scanning Tunneling Microscopy II*; Springer Verlag: New York, 1992.

(37) Tromp, R. M.; Van Loenen, E. J.; Demuth, J. E.; Lang, N. D. *Phys. Rev B.* **1988**, *37*, 9042−9053.

(38) Hamers, R. J. *Ann. Rev. Phys. Chem.* **1989**, *40*, 531−559.

(39) Lindsay, S.; Sankey, O. F.; Li, Y.; Herbst, C.; Rupprecht, A. *J. Phys. Chem.* **1990**, *94*, 4655−4660.

(40) Eigler, D. M.; Weiss, P. S.; Schweizer, E. K.; Lang, N. D. *Phys. Rev. Lett.* **1991**, *66*, 1189−1194.

(41) Maroie, S.; Savy, M.; Verbist, J. *J. Inorg. Chem.* **1979**, *1*, 2560−2567.

(42) Wagonerova, D. M.; Schwertnerova, E.; Veprek-siska, J. *Colloid Chem. Commun.* **1974**, *39*, 1981−1989.

(43) Gruen, L. C.; Blagrove, R. J. *Aust. J. Chem.* **1973**, *26*, 319−322.

(44) Szuber, J.; Szczepaniak, B.; Kochowski, S.; Opilski, A. *Vacuum* **1995**, *46*, 547−549.

(45) Dahlberg, S. C.; Musser, M. E. *J. Chem. Phys.* **1980**, *72*, 6706−6711.